RESULTS FROM THE CHORUS EXPERIMENT

Maria-Gabriella Catanesi
CERN
Geneva, Switzerland

Representing the CHORUS Collaboration

ABSTRACT

The recent results from the CHORUS experiment are summarised.
CHORUS is an experiment made to study the neutrino oscillation using the pure and intense ν_μ Wide Beam at SPS(CERN).
A fraction of the neutrino interactions collected during the years 1994-1995 and 1996 by the CHORUS experiment has been analysed, searching for ν_τ charged current interactions followed by the τ lepton decay into a negative hadron or into a muon. Within the applied cuts, no ν_τ candidate has been found.
This result leads to a 90% C.L. limit $P(\nu_\mu \rightarrow \nu_\tau) < 6.0 \cdot 10^{-4}$ on the mixing probability.
We also report about the first direct observation of a neutrino induced charged current interation with two subsequent decays of short-lived particles that a complete analysis allows to interpreter as D_s^{+*} production followed by the decay chain $D_s^{+*} \rightarrow D_s^+\gamma, D_s^+ \rightarrow \tau^+\nu_\tau, \tau^+ \rightarrow \mu^+\nu_\mu\bar{\nu_\tau}$.

1 Introduction

The question about the neutrino mass and stability remains one of the most interesting in the actual physics scenario . This question is particulary relevant for the ν_τ ,as member of the third generation family of fermions, one of the most promising candidate for the dark matter in the universe.

Stimulated by these considerations a new generation of accelerator experiments was build in order to search ,with improved sensitivities , the $\nu_\mu \rightarrow \nu_\tau$ oscillation[1].[2]

The approch adopted by the CHORUS experiment was to use a visual technique that allows a direct observation of the τ decay topology.

The experiment was taking data since april 94 to september 1997 in the reoptimized and rebuild CERN Wide Band ν_μ.[3]

The new beam present a higher intensity ($> 2 \times 10^{13}$ protons/cycle) and a higher mean neutrino energy ($< E_{\nu_\mu} > \approx 27$ GeV) . The mean distance of the neutrino source from the detector is 600 m. This together with the events statistics and background fixes the sensitivity of the experiment.

The aim is to explore mixing angles down to $sin^2(2\theta) \sim 10^{-4}$ putting ,in case of absence of signal, a new limit a factor 20 better of the existing one .[5]

2 The Detector

CHORUS is a "classic" appearance experiment. In fact was conceived to identify ν_τ detecting the τ path and decay vertex.

In particular the aim is isolate "few" signal events coming from the charge current interactions:

$$\nu_\tau N \rightarrow \tau^- X$$

followed by one of the decay topologies:

$$\begin{array}{lll} \tau^- & \hookrightarrow \mu^- \nu \nu & 18\% \\ & \hookrightarrow h^- \nu + n\pi^0 & 50\% \\ & \hookrightarrow h^- h^- h^+ + n\pi^0 & 14\% \end{array}$$

From the large background of charged and neutral current interactions:

$$\nu_\mu N \rightarrow \mu^- X$$
$$\nu_\mu N \rightarrow \nu_\mu X$$

Because of the very short τ^- decay length (cτ=90μm) we need a precise device like nuclear emulsions that provide the required high spacial resolution in the micron range. The CHORUS target was made by 800 Kg of emulsion gel segmented in four stacks of 1 radiation lenght each. Each stack is subdivided in 36 sheets. This configuration allows fast automatic and semiautomatic scanning techniques [5] (developed at the Nagoya university) that permit to speed-up the search time.
A further improuvement can be obtained reducing the scanning area. This goal is reached introducing between the emulsion stacks a scintillating fibre tracking detector that predict the tracks position at the stack exit.[6]
The detection of long lived particles is done in CHORUS using two magnetic spec-

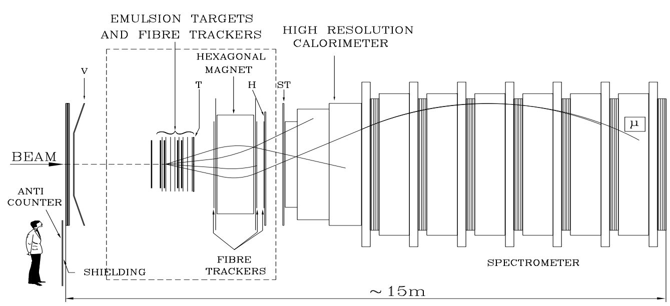

Figure 1: The CHORUS detector

trometers and a calorimeter (see fig 1).
The first spectrometer, placed downstream of the target, consist in an array of three diamond-shaped fiber planes in a magnetic field of 0.12T generated by a hexagonal air-core magnet[7] operating in pulsed mode, that allows to determine sign and momentum of low energy particles (below 10GeV).
The second one, placed downstream of the calorimeter, is a “classic” muon spectrometer that allows to measure the momentum with a resolution of 20% at 75 GeV/c for muons up to 100 GeV/c. It consist of six circulary magnetisated iron modules with a magnetic field of 1.8T interlived with tracking section composed by drift chambers and streamer tube planes. The CHORUS calorimeter is the first large-scale application of

Table 1: *Current status of the CHORUS analysis*

	1994	1995	1996
Protons on target	$0.81 \cdot 10^{19}$	$1.20 \cdot 10^{19}$	$1.38 \cdot 10^{19}$
Emulsion triggers	422,000	547,000	617,000
1μ to be scanned	66,911	110,916	129,669
0μ to be scanned	17,731	27,841	32,548
1μ scanned so far	42,154	49,912	72,615
0μ scanned so far	8,908	12,635	-
1μ vertex located	18,286	20,642	30,128
0μ vertex located	3,401	3,805	0

the so called "spaghetti tecnique"[8] . It consist of a sampling of lead and scintillating fiber matrix optimized for compensation, with an equal response to electromagnetic and hadronic showers.

A full description of the CHORUS detector can be found in .[9]

3 Data selection and analysis

3.1 Data collection and selection criteria

In the 1994-1997 period, CHORUS has collected 2,271,000 triggers corresponding to $5.06\ 10^{19}$ protons on target. Of these, 458,601 have a muon identified in the final state (the so called 1μ events) and 116,049 do not (the so called 0μ events) and a vertex position compatible with one of the four emulsion target stacks.

All tracks, associated to the interaction vertex, with an angle less than 0.4 rad with the beam axis and, in view of the large emulsion background of muons originating from a nearby secondary target, bigger than 0.05 rad from the direction of this target are extrapolated downstream and selected for further analysis. These tracks are searched for in the emulsion if their charge is negative and their momentum is in the range $0 \leq p_h \leq 20$ GeV/c and $0 \leq p_\mu \leq 30$ GeV/c for hadrons and muons, respectively.

3.2 Vertex location in emulsion

The various steps leading to the plate containing the vertex by means of fully automatised microscopes are identical to those described in.[10,11] They are independently applied to all the selected tracks in the event, the muon for the 1μ events, all the negative tracks for the 0μ events. A track which has been found in the interface emulsion sheets is followed upstream in the target emulsion, using track segments reconstructed in the most upstream 100 μm of each plate, until the track disappears. This plate is referred to as the vertex plate.

The mean efficiency of this scan-back procedure is found to be $\sim 32\%$ and $\sim 42\%$ for 0μ and 1μ events, respectively. The scanning results are summarised in Table 1.

3.3 Decay search

Once the vertex plate is defined, automatic microscope measurements are performed to select the events potentially containing a decay topology (kink). Different algorithms have been applied, as a result of the progress in the scanning procedures and of the improving performance in speed of the scanning devices. They are described in[10,11] and briefly recalled here.

In the first procedure the event is selected either when the scan-back track has a significant impact parameter with respect to the other predicted tracks or when the change in the scan-back track direction between the vertex plate and the exit from the emulsion corresponds to an apparent transverse momentum, p_T, larger than 250 MeV/c. For the selected events and for those with only one predicted track, digital images of the vertex plate are recorded and are analysed off-line for the presence of a kink.

The second procedure is restricted to the search of *long* decay paths. In that case the vertex plate is assumed to contain the decay vertex of a charged parent particle produced in a more upstream plate. With this procedure only kink angles larger than 0.025 rad are detected.

For the events selected by either one of these procedures, a computer assisted eye-scan is performed to assess the presence of a secondary vertex and measure accurately its topology. A τ^- decay candidate must satisfy the following criteria:

1. the secondary vertex appears as a kink without black prongs, nuclear recoils, blobs or Auger electrons;

2. the transverse momentum of the decay muon (hadron) with respect to the parent direction is larger than 250 MeV/c (to eliminate decays of strange particles);
3. the kink, in the 0μ channel, occurs within 3 plates downstream from the neutrino interaction vertex plate. Because of the lower background, the kink search in the muonic decay channel was extended to 5 plates, with a gain in efficiency of about 8%.

No τ^- decay candidate has been found satisfying the selection criteria.

3.4 Background estimates

In this section we discuss the expected background from known sources for both hadronic and muonic τ decay channels.

Sources of background for the hadronic τ decay channel are:

- the production of negative charmed particles from the anti-neutrino components of the beam. These events constitute a background if the primary μ^+ or e^+ remains unidentified. We expect ~ 0.02 events from these sources;
- the production of positive charmed mesons in charged current interactions, if the primary lepton is not identified and the charge of the charmed particle daughter is incorrectly measured. We expect ~ 0.03 events from this source in the present sample;
- the associated charm production both in charged (when the primary muon is lost) and neutral current interactions, when one of the charmed particles is not detected. In the present sample, the estimated background from this process taking into account the total charged current cross-section [12] and the upper limit production rate of associated charm in charged current interactions is < 0.01 events.
- the main potential background to the hadronic τ^- decays is due to so-called hadronic "white kinks", defined as 1-prong nuclear interactions with no heavily ionising tracks (*black* and *grey* tracks in emulsion terminology) and no evidence for nuclear break up (evaporation tracks, recoils, blobs or Auger electrons). Published data allowing to determine the white kink interaction cross-section are scarce.[13,14] The main source is a dedicated experiment with 4 GeV pions at KEK.[13]

Since the experimental information of the p_T dependence is statistically poor at large values, a Monte Carlo simulation, based on a modified version of FLUKA[15,16] has been performed. The results of this simulation are in good agreement with the p_T dependence of the KEK measurement. We estimate with the current statistic a background of 0.5 events within 3 plates downstream from the primary vertex plate.

The main source of potential background in the muonic τ channel is the charm production. We expect less than 0.1 events in the current sample from the anti-neutrino components of the beam:

$$\bar{\nu}_\mu(\bar{\nu}_e)M \rightarrow \mu^+(e^+)D^-X$$

followed by

$$D^- \rightarrow \mu^- X^0$$

in which the $\mu^+(e^+)$ escapes the detection or is not identified.

The prompt ν_τ contamination of the beam[17] is a background common to both the hadronic and muonic decay channels. For the present sample the expected background is much less than 0.1 events.

4 Results

4.1 Oscillation sensitivity

In the usual approximation of a two-flavour mixing scheme, the probability of ν_τ appearance in an initially pure ν_μ beam can be expressed as

$$\begin{aligned} P_{\mu\tau}(E) &= \sin 2t \cdot \int \Psi(E,L) \cdot \\ &\cdot sin^2\left(\frac{1.27 \cdot \Delta m^2_{\mu\tau}(eV^2) \cdot L(km)}{E(GeV)}\right) \cdot dL \end{aligned}$$

where

- E is the incident neutrino energy;

Table 2: *Quantities used in the estimation of the sensitivity*

	1994	1995	1996
N_μ	18,286	20,642	30,128
r_σ	1.89	1.89	1.89
r_A	0.93	0.93	0.93
$\langle A_{\tau\mu}\rangle$	0.39	0.39	0.39
$\langle A_{\tau h}\rangle$	0.17	0.17	-
$\langle A_{\tau e}\rangle$	0.093	0.093	-
$\langle A_{\tau\bar{\mu}}\rangle$	0.026	0.026	-
$\langle \epsilon_{\tau\mu}\rangle$	0.53	0.35	0.37
$\langle \epsilon_{\tau h}\rangle$	0.24	0.25	-
$\langle \epsilon_{\tau e}\rangle$	0.12	0.13	-
$\langle \epsilon_{\tau\bar{\mu}}\rangle$	0.22	0.23	-
N_μ^{eq}	11,987	12,743	-

- L is the neutrino flight length to the detector;
- $\theta_{\mu\tau}$ is the effective $\nu_\mu - \nu_\tau$ mixing angle;
- $\Delta m^2_{\mu\tau}$ is the difference of the squared masses of the two assumed mass eigenstates;
- $\Psi(E, L)$ is the fraction of ν_μ with energy E originating at a distance between L and $L + dL$ from the emulsion target.

The τ^- channels considered in the $\nu_\mu \rightarrow \nu_\tau$ oscillation search we describe in this paper are:

1) $\tau \rightarrow \mu$, 2) $\tau \rightarrow h$, 3) $\tau \rightarrow e$ and 4) $\tau \rightarrow \bar{\mu}$ (the μ is not identified) channels.

The expected number, $N_{\tau i}$ ($i = 1, 2, 3, 4$), of observed τ^- decays into a channel of branching ratio BR_i is then given by

$$N_{\tau i} = BR_i \cdot \int \Phi_{\nu_\mu} \cdot P_{\mu\tau} \cdot \sigma_\tau \cdot A_{\tau i} \cdot \epsilon_{\tau i} \cdot dE \tag{1}$$

with

- $BR_{(1\ or\ 4)} = BR(\tau \rightarrow \nu_\tau \bar{\nu}_\mu \mu^-) = (17.35 \pm 0.10)\%$[18]).

- $BR_2 = BR(\tau \to \nu_\tau h^- n h^0) = (49.78 \pm 0.17)\%$[18];
- $BR_3 = BR(\tau \to \nu_\tau \bar{\nu}_e e^-) = (17.83 \pm 0.08)\%$[18];
- Φ_{ν_μ} the incident ν_μ flux spectrum;
- σ_τ the charged current ν_τ interaction cross-section;
- $A_{\tau i}$ the acceptance and reconstruction efficiency for the considered channel (up to the vertex plate location);
- $\epsilon_{\tau i}$ the corresponding efficiency of the decay search procedure;

With proper averaging (denoted by $\langle\rangle$), $N_{\tau i}$ can also be written as a function of n_i:

$$N_{\tau i} = BR_i \cdot n_i \cdot \langle P_{\mu\tau} \rangle \cdot \frac{\langle \sigma_\tau \rangle}{\langle \sigma_\mu \rangle} \cdot \frac{\langle A_{\tau i} \rangle}{\langle A_\mu \rangle} \cdot \langle \epsilon_{\tau i} \rangle \tag{2}$$

where

- $n_1 = N_\mu$ (the number of located charged current ν_μ interactions corresponding to the considered event sample) and $n_2 = n_3 = n_4 = (N_\mu)_{0-\mu}$ (the product of N_μ and the relative fraction of the 0-μ sample for which the analysis has been completed);
- $\langle \sigma_{\mu(\tau)} \rangle = \int \frac{d\sigma_{\mu(\tau)}}{dE} \cdot \Phi_{\nu_\mu} \cdot dE$. It takes into account quasi-elastic interactions, resonance production and deep inelastic interactions ($\sigma(\frac{\langle \sigma_\tau \rangle}{\langle \sigma_\mu \rangle})_{syst} \sim 7\%$);
- $\langle A_{\mu(\tau i)} \rangle = \int \frac{d\sigma_{\mu(\tau)}}{dE} \cdot A_{\mu(\tau i)} \cdot \Phi_{\nu_\mu} \cdot dE$ ($\sigma(\frac{\langle A_{\tau i} \rangle}{\langle A_\mu \rangle})_{syst} \sim 7\%$);
- $\langle \epsilon_{\tau i} \rangle$ is the average efficiency of the decay search procedure for the accepted events ($\sigma(\langle \epsilon_{\tau i} \rangle)_{syst} \sim 10\%$);

To allow an easy combination of the results from the 1-μ and 0-μ event samples, it is useful to define the “equivalent number of muonic events” of the 0-μ sample by

$$N_\mu^{eq} = (N_\mu)_{0-\mu} \cdot \sum_{i=2}^{4} \frac{\langle A_{\tau i} \rangle}{\langle A_{\tau\mu} \rangle} \cdot \frac{\langle \epsilon_{\tau i} \rangle}{\langle \epsilon_{\tau\mu} \rangle} \cdot \frac{BR_i}{BR_\mu} \tag{3}$$

The 90% C.L. upper limit on the oscillation probability then simplifies to

$$P_{\mu\tau} \leq \frac{2.38 \cdot r_\sigma \cdot r_A}{BR_\mu \cdot \langle \epsilon_{\tau\mu} \rangle \cdot [N_\mu + N_\mu^{eq}]} \tag{4}$$

where $r_\sigma = \langle \sigma_\mu \rangle / \langle \sigma_\tau \rangle$ and $r_A = \langle A_\mu \rangle / \langle A_{\tau\mu} \rangle$.

In the above formula, the numerical factor 2.38 takes into account the total systematic error (17%) following the prescription given in.[19] The systematic error is mainly due to the reliability of the Monte Carlo simulation of the scanning procedures.

The estimated values of the quantities appearing in this expression are given in Table 2. No statistical errors are quoted since they are much smaller than the systematic uncertainty.

Using the present sample the following 90% C.L. limit is obtained

$$P_{\mu\tau} \leq 6.0 \cdot 10^{-4} \tag{5}$$

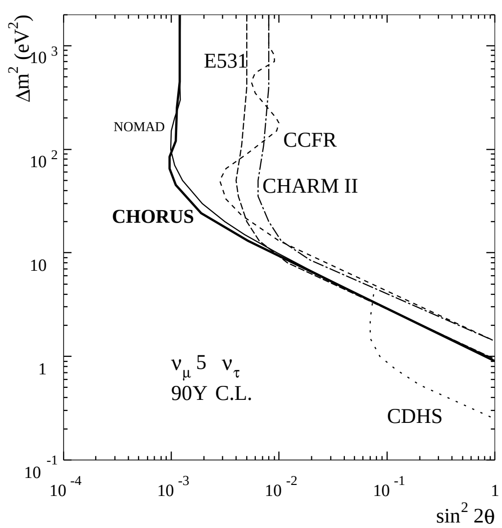

Figure 2: Present result compared with the recent NOMAD result[20] (full line) and the previous limits (dotted lines).

In a two flavour mixing scheme, the 90% C.L. excluded region in the ($\sin 2t$, $\Delta m^2_{\mu\tau}$) parameter space is shown in Figure 2. Maximum mixing between ν_μ and ν_τ is excluded at 90% C.L. for $\Delta\ m^2_{\mu\tau}\ \ > 0.9$ eV^2; the large Δm^2 are excluded at 90% C.L. for $\sin 2t > 1.2 \cdot 10^{-3}$.

4.2 The D_s^{+*} observation

We have observed a neutrino induced charged current interaction with two subsequent decays within $215\mu m$. A complete analysis of this event is possible because of the exceptional tracking capabilities of the CHORUS emulsion detector. Topological and kinematical reconstruction for the complete event are consistent with the decay chain

$$
\begin{array}{llll}
\nu_\mu\, n \longrightarrow \mu^- D_s^{+*} n & & & \\
\quad\quad\quad\ \ \llcorner\!\!\longrightarrow D_s^+ \gamma & & & \\
\quad\quad\quad\quad\quad\quad\ \llcorner\!\!\longrightarrow \tau^+ \nu_\tau & & & \\
\quad\quad\quad\quad\quad\quad\quad\quad\ \ \llcorner\!\!\longrightarrow \mu^+ \nu_\mu \bar{\nu}_\tau & & &
\end{array}
$$

To find double kink events from the reaction $\nu_\mu N \to \mu^- D_s^+(^* \to D_s^+\gamma)(X^0),\ D_s^+ \to \tau^+\nu_\tau, \tau^+ \to \mu^+\nu_\mu\bar{\nu_\tau}$, events with two opposite sign muons in the electronic detector are selected. To be sensitive to $D_s^{+*} \to D_s\gamma$ decays, we allow only electromagnetic energy in the calorimeter and veto on hadronic activity. After finding the primary vertex the event signature is examined manually for decay topologies with a double kink.

One event recorded in the 1994 exposure fulfills all requirements of this event selection (see fig 3).

In view of the short flight lengths with the measured momenta and decay angles, we assume the neutrino induced production of a charmed particle (D or D_s meson) at the primary vertex. The probabilities for the different scenarios to happen and being detected in the CHORUS detector have been studied. The decay chain $D_s \to \tau \to \mu$ is clearly favoured. Furthermore, the measured decay angles and momenta of the candidate event are consistent with this hypothesis.

Therefore, we may conclude that the observed double kink originates from the signature of $D_s^+ \to \tau^+\nu_\tau$, $\tau^+ \to \mu^+\nu_\mu\bar{\nu_\tau}$.

At the primary vertex no nuclear break up is observed. Low $Q^2 = (0.77{\pm}0.15)\ (GeV/c)^2$ and the signal of a recoil neutron ($t = (0.89 \pm 0.39)\ (GeV/c)^2$) point to a diffractive D_s^* production .

5 Conclusions

The emulsion scanning methods, previously described in,[10,11] have been applied to a fraction of the 1994-1995-1996 data. No τ^- decay candidate has been found, leading to a more stringent 90% C.L. upper limit on the $\nu_\mu \to \nu_\tau$ oscillation probability

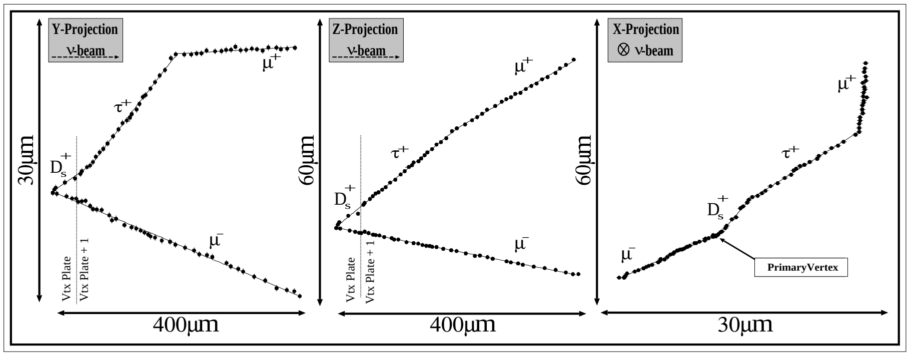

Figure 3: The double kink event in the emulsion

($P_{\mu\tau} \leq 6.0 \cdot 10^{-4}$). During the second phase of the analysis (with better efficiencies, larger statistics and faster automatic emulsion scanning) we plan to reach the design sensitivity $(P_{\mu\tau} \leq 1.0 \cdot 10^{-4})$.[1] The first direct observation of a neutrino induced charged current interaction with a D_s^{+*} production detected at the vertex prove the exceptional capability of CHORUS in the detection of rare process involving decay of short live particles.

References

[1] CHORUS Collaboration, A new search for $\nu_\mu \to \nu_\tau$ CERN/PPE/93-131

[2] NOMAD Collaboration proposal

[3] G.Aquistapace *et al.*,The West Area Neutrino Facility for CHORUS and NOMAD experiments:"94 to 97 operations", CERN/ECP/95-14

[4] N.Ushida *et al.*(E531),Phys.Rev.Lett.,57 (1986) 2897.

[5] S. Aoki *et al.*,Fully Automated Emulsion Analysis System, NIM B51 (1990) 466.

[6] S. Aoki *et al.*,Scintillating fiber tracker with opto-electronics readout for the CHORUS neutrino experiment,NIM A344 (1994) 254.

[7] F. Bergsma *et al.*, The hexagonal toroidal air-core magnet of the CHORUS detector,NIM A357 (1995) 243.

[8] S. Buontempo *et al.*, Response to electrons and pions of the calorimeter for the CHORUS experiment CERN-PPE/96-188 Nucl. Instr. and Meth. **A378** 222 (1996)

[9] E. Eskut *et al.*, CHORUS Collaboration, Nucl. Instr. and Meth. **A401** 7 (1997).

[10] E. Eskut *et al.*, CHORUS Collaboration, Phys. Lett. B 424 (1998) 202.

[11] E. Eskut *et al.*, CHORUS Collaboration, CERN-EP/98-73. Accepted for publication on Phys. Lett. B.

[12] N. Ushida *et al.*, E531 Collaboration, Phys. Lett. **B206** 375 (1988).

[13] K. Kodama *et al.*, FERMILAB P803 Proposal (1993), Appendix D.

[14] F. Baldassarre *et al.*, Nuovo Cimento XXI, 3 (1961) 459.

[15] A. Fassò, A. Ferrari, J. Ranft and P.R. Sala, "New developments in FLUKA modelling of hadronic and EM interactions", in Proceedings of the 3rd workshop on "Simulating Accelerator Radiation Environment", SARE-3, KEK-Tsukuba, May 7–9 1997, H. Hirayama ed., KEK report Proceedings 97-5, p. 32 (1997).

[16] A. Ferrari, T. Rancati and P.R. Sala, "FLUKA applications in high energy problems: from LHC to ICARUS and atmospheric showers", in Proceedings of the 3rd workshop on "Simulating Accelerator Radiation Environment", SARE-3, KEK-Tsukuba, May 7–9 1997, H. Hirayama ed., KEK report Proceedings 97-5, p. 165 (1997).

[17] B. Van de Vyver, Nucl. Instr. and Meth. **A385** 91 (1997).

[18] Particle Data Group, Phys. Rev. **D54** 1 (1996).

[19] R.D. Cousins and V.L. Highland, Nucl. Instr. and Meth. **A320** 331 (1992).

[20] A. Marchionni for the NOMAD Collaboration, these Proceedings